

hep-ph/0303043

CERN-TH/2003-051

UMN-TH-2132/03

TPI-MINN-03/07

Supersymmetric Dark Matter in Light of WMAP

John Ellis¹, Keith A. Olive², Yudi Santoso² and Vassilis C. Spanos²

¹*TH Division, CERN, Geneva, Switzerland*

²*William I. Fine Theoretical Physics Institute,
University of Minnesota, Minneapolis, MN 55455, USA*

Abstract

We re-examine the parameter space of the constrained minimal supersymmetric extension of the Standard Model (CMSSM), taking account of the restricted range of $\Omega_{CDM}h^2$ consistent with the WMAP data. This provides a significantly reduced upper limit on the mass of the lightest supersymmetric particle LSP: $m_\chi \lesssim 500$ GeV for $\tan\beta \lesssim 45$ and $\mu > 0$, or $\tan\beta \lesssim 30$ and $\mu < 0$, thereby improving the prospects for measuring supersymmetry at the LHC, and increasing the likelihood that a 1-TeV linear e^+e^- collider would be able to measure the properties of some supersymmetric particles.

CERN-TH/2003-051

March 2003

1 Introduction

The recent data from the WMAP satellite [1] confirm with greater accuracy the standard cosmological model, according to which the current energy density of the Universe is comprised by about 73 % of dark energy and 27 % of matter, most of which is in the form of non-baryonic dark matter. The WMAP data further tell us that very little of this dark matter can be hot neutrino dark matter, and the reported re-ionization of the Universe when the redshift $z \sim 20$ is evidence against warm dark matter. WMAP quotes a total matter density $\Omega_m h^2 = 0.135_{-0.009}^{+0.008}$ and a baryon density $\Omega_b h^2 = 0.0224 \pm 0.0009$ [1], from which we infer the following $2\text{-}\sigma$ range for the density of cold dark matter: $\Omega_{CDM} h^2 = 0.1126_{-0.0181}^{+0.0161}$. This range is consistent with that inferred from earlier observations [2, 3], but is significantly more precise.

It has been appreciated for some time that the lightest supersymmetric particle (LSP) is a suitable candidate for this non-baryonic cold dark matter [4]. The LSP is stable in supersymmetric models where R parity is conserved, and its relic density falls naturally within the favoured range if it weighs less than ~ 1 TeV. This statement may be made more precise in the minimal supersymmetric extension of the Standard Model (MSSM), in which the LSP is expected to be the lightest neutralino χ , particularly if the soft supersymmetry-breaking mass terms $m_{1/2}, m_0$ are constrained to be universal at an input GUT scale: the constrained MSSM (CMSSM). Since $\Omega_\chi h^2 \propto m_\chi n_\chi$, where n_χ is the relic LSP number density, and n_χ typically increases as the universal soft supersymmetry-breaking mass parameters are increased, one would expect the upper limit on m_χ to *decrease* when the upper limit on $\Omega_{CDM} h^2$ is *decreased*. Compared with taking this upper limit to be 0.3, as we and others [5, 6, 7] have done previously, taking $\Omega_{CDM} h^2 < 0.129$ as suggested by the WMAP data - which is line with estimates from previous CMB determinations used in [8] - may therefore be expected to improve significantly the corresponding upper limit on m_χ .

Such is indeed the case for $\tan\beta \lesssim 45$ and $\mu > 0$, or for $\tan\beta \lesssim 30$ and $\mu < 0$, as we show below, where the largest values of m_χ are found in the $\chi - \tilde{\tau}$ coannihilation region. We find for these cases that $m_{1/2} \lesssim 900 - 1200$ GeV for $\Omega_{CDM} h^2 < 0.129$, whereas $m_{1/2} \lesssim 1400 - 1750$ GeV would have been allowed for $\Omega_{CDM} h^2 < 0.3$. Correspondingly, the upper limit on the LSP mass becomes $m_\chi \lesssim 400 - 500$ GeV, rather than $m_\chi \lesssim 600 - 700$ GeV as found previously [9, 10]. This stronger upper limit improves the prospects for measuring supersymmetry at the LHC. Also, it would put sleptons within reach of a 1-TeV linear e^+e^- linear collider, whereas previously a centre-of-mass energy above 1.2 TeV might have appeared necessary [11]. All the above remarks would also apply if other particles also

contribute to Ω_{CDM} .

For any fixed value of $\tan\beta$ and sign of μ , only a narrow region of CMSSM parameter space would be allowed if $0.094 < \Omega_\chi h^2 < 0.129$, as would be implied by WMAP if there are no other significant contributors to the density of cold dark matter. The previous ‘bulk’ regions of parameter space at small values of m_0 and $m_{1/2}$ now become quite emaciated, and the previous coannihilation strips now become much narrower, as do the rapid-annihilation funnels that appear at larger $\tan\beta$ [12, 5]. However, unlike the coannihilation strips, the rapid-annihilation funnels still extend to very large values of m_0 and $m_{1/2}$, the absolute upper limit on m_χ is much weaker for $\tan\beta \gtrsim 50$ if $\mu > 0$, or for $\tan\beta \gtrsim 35$ if $\mu < 0$ ¹. The narrowness of the preferred region implies that $\tan\beta$ could in principle be determined from measurements of $m_{1/2}$ and m_0 , as we discuss later.

2 WMAP Constraint on the CMSSM Parameter Space

Fig. 1 displays the allowed regions of the CMSSM parameter space for (a) $\tan\beta = 10, \mu > 0$, (b) $\tan\beta = 10, \mu < 0$, (c) $\tan\beta = 35, \mu < 0$, and (d) $\tan\beta = 50, \mu > 0$. We have taken $m_t = 175$ GeV and $A_0 = 0$ in all of the results shown below. In each panel, we show the regions excluded by the LEP lower limits on $m_{\tilde{e}}, m_{\chi^\pm}$ and m_h , as well as those ruled out by $b \rightarrow s\gamma$ decay [14] as discussed in [15]. In panels (a) and (d) for $\mu > 0$, we also display the regions favoured by the recent BNL measurement [16] of $g_\mu - 2$ at the $2\text{-}\sigma$ level, relative to the calculation of the Standard Model based on e^+e^- data at low energies [17].

Also shown in Fig. 1 are the ‘old’ regions where $0.1 < \Omega_\chi h^2 < 0.3$, and the ‘new’ regions where $0.094 < \Omega_\chi h^2 < 0.129$. We see immediately that (i) the cosmological regions are generally much narrower, and (ii) the ‘bulk’ regions at small $m_{1/2}$ and m_0 have almost disappeared, in particular when the laboratory constraints are imposed. Looking more closely at the coannihilation regions, we see that (iii) they are significantly truncated as well as becoming much narrower, since the reduced upper bound on $\Omega_\chi h^2$ moves the tip where $m_\chi = m_{\tilde{\tau}}$ to smaller $m_{1/2}$. It is this effect that provides the reduced upper bound on m_χ advertized earlier. In panels (c) and (d), we see rapid-annihilation funnels that (iv) are also narrower and extend to lower $m_{1/2}$ and m_0 than previously. They weaken significantly the upper bound on m_χ for $\tan\beta \gtrsim 35$ for $\mu < 0$ and $\tan\beta \gtrsim 50$ for $\mu > 0$.

We take this opportunity to comment on some calculational details concerning the rapid-annihilation funnels. Comparison with other studies of these regions [7, 18] has shown the

¹Strictly speaking, there is also a filament of parameter space extending to large m_χ in the ‘focus-point’ region [13] at large m_0 , to which we return later.

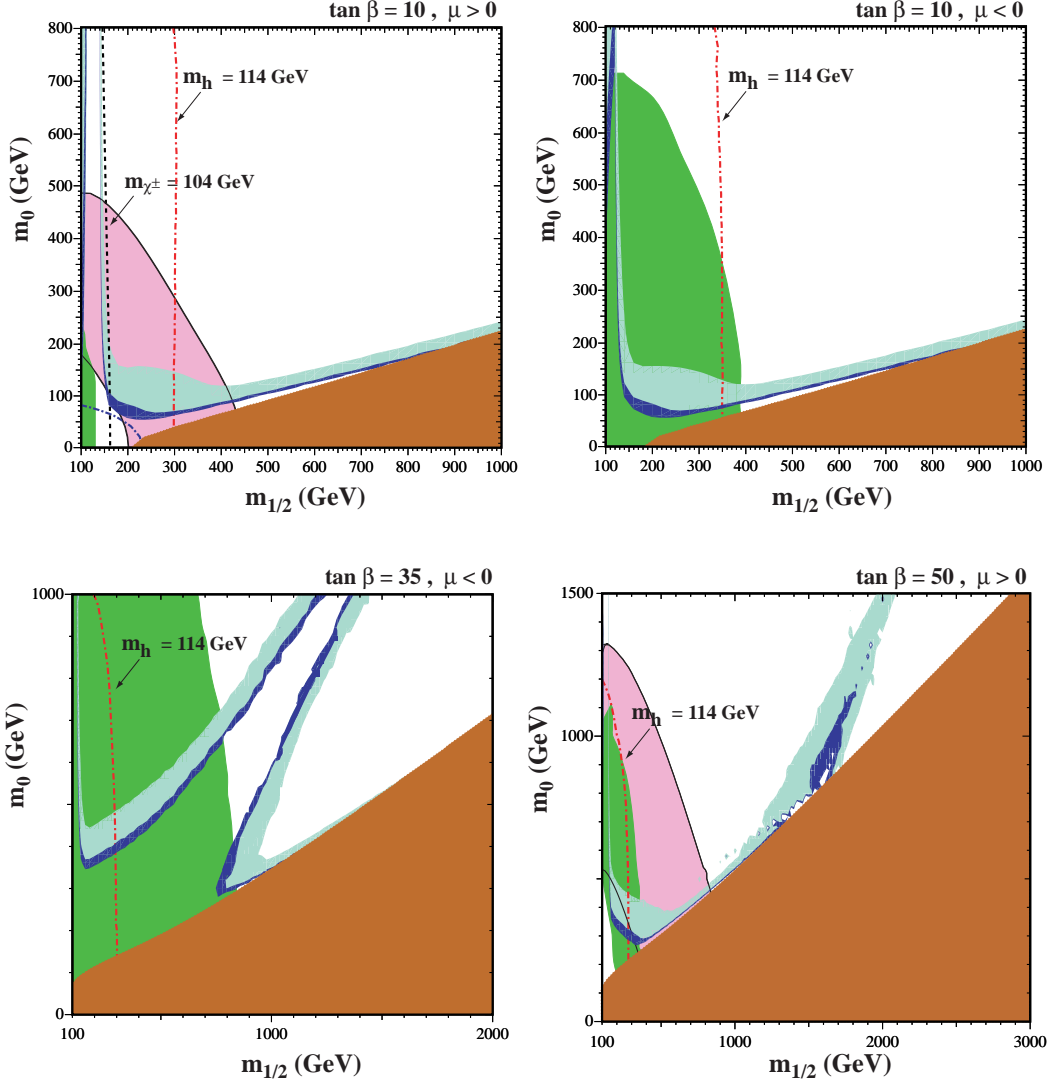


Figure 1: The $(m_{1/2}, m_0)$ planes for (a) $\tan \beta = 10, \mu > 0$, (b) $\tan \beta = 10, \mu < 0$, (c) $\tan \beta = 35, \mu < 0$, and (d) $\tan \beta = 50, \mu > 0$. In each panel, the region allowed by the older cosmological constraint $0.1 \leq \Omega_\chi h^2 \leq 0.3$ has medium shading, and the region allowed by the newer cosmological constraint $0.094 \leq \Omega_\chi h^2 \leq 0.129$ has very dark shading. The disallowed region where $m_{\tilde{\tau}_1} < m_\chi$ has dark (red) shading. The regions excluded by $b \rightarrow s\gamma$ have medium (green) shading, and those in panels (a,d) that are favoured by $g_\mu - 2$ at the $2\text{-}\sigma$ level have medium (pink) shading. A dot-dashed line in panel (a) delineates the LEP constraint on the \tilde{e} mass and the contours $m_{\chi^\pm} = 104$ GeV ($m_h = 114$ GeV) are shown as near-vertical black dashed (red dot-dashed) lines in panel (a) (each panel).

importance of treating correctly the running mass of the bottom quark, as we have done in previous works [5]. Also important is the correct treatment of annihilation rates across the convolution of two Boltzmann distributions when the cross section varies rapidly, as in the rapid-annihilation funnels, and we have taken the opportunity of this paper to improve our previous treatment. The results on the low- $m_{1/2}$ sides of the the rapid-annihilation funnels are indistinguishable from those shown previously, apart from the narrowing due to the smaller allowed range of $\Omega_\chi h^2$. However, there are more significant differences on the high- $m_{1/2}$ sides of the the rapid-annihilation funnels, where our previous approximation was less adequate. This is most noticeable for the case $\tan\beta = 50, \mu > 0$ shown in panel (d) of Fig. 1, where the two strips with relic density in the allowed range are all but merged. A second side of the rapid-annihilation funnel becomes distinctly visible when $\tan\beta \geq 51$, but the gap between the two sides is much narrower than we found previously. This is also true for $\mu < 0$, and is exemplified in Fig. 1c for $\tan\beta = 35$ where both sides of the funnel region are clearly distinct².

Before discussing further our results, we comment on the potential impact of a re-evaluation of m_t . A recent re-analysis by the D0 collaboration favours a central value some 5 GeV higher than the central value $m_t = 175$ GeV that we use [19]. If confirmed, this would shift the displayed contours of $m_h = 114$ GeV to lower $m_{1/2}$, e.g., from $m_{1/2} \simeq 300$ GeV to $m_{1/2} \simeq 235$ GeV in the case $\tan\beta = 10, \mu > 0$. This would not affect the upper bound on m_χ that we quote later, but it would weaken the lower limit on m_χ in cases where this is provided by the LEP Higgs limit.

The focus-point region would, however, be affected spectacularly by any such increase in m_t , shifting to much larger m_0 . In the analysis of [13], for $\tan\beta = 10$ and $m_{1/2} = 300$ GeV, the focus-point is pushed up from $m_0 \simeq 2200$ GeV to $m_0 \simeq 4200$ GeV when m_t is increased from 175 GeV to 180 GeV, and for $\tan\beta = 50$, it is pushed up from $m_0 \simeq 1800$ GeV to $m_0 \simeq 3000$ GeV. In our treatment of the CMSSM, we in fact find no focus-point region when $m_t = 180$ GeV. In view of this instability in the fixed-point region, we do not include it in our subsequent analysis: our limits should be understood as not applying to this region, though we do note that it would also be further narrowed by the more restricted range of $\Omega_\chi h^2$.

We display in Fig. 2 the strips of the $(m_{1/2}, m_0)$ plane allowed by the new cosmological constraint $0.094 < \Omega_\chi h^2 < 0.129$ and the laboratory constraints listed above, for $\mu > 0$ and values of $\tan\beta$ from 5 to 55, in steps $\Delta(\tan\beta) = 5$. We notice immediately that the strips

²Note that the irregularities seen in the cosmological regions are a result of the resolution used to produce the figures.

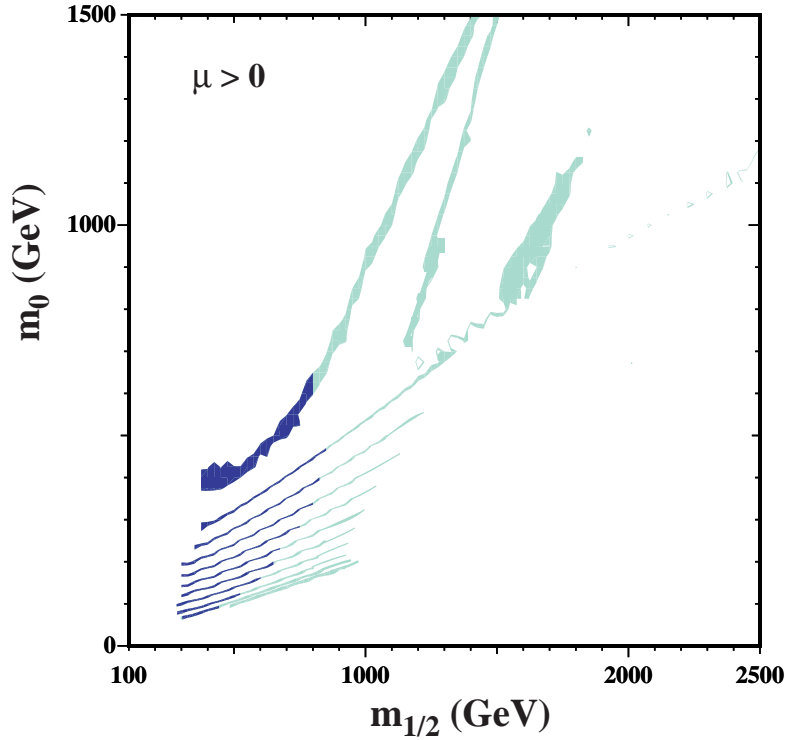


Figure 2: *The strips display the regions of the $(m_{1/2}, m_0)$ plane that are compatible with $0.094 < \Omega_\chi h^2 < 0.129$ and the laboratory constraints for $\mu > 0$ and $\tan\beta = 5, 10, 15, 20, 25, 30, 35, 40, 45, 50, 55$. The parts of the strips compatible with $g_\mu - 2$ at the $2\text{-}\sigma$ level have darker shading.*

are considerably narrower than the spacing between them, though any intermediate point in the $(m_{1/2}, m_0)$ plane would be compatible with some intermediate value of $\tan\beta$. The right (left) ends of the strips correspond to the maximal (minimal) allowed values of $m_{1/2}$ and hence m_χ ³. The lower bounds on $m_{1/2}$ are due to the Higgs mass constraint for $\tan\beta \leq 23$, but are determined by the $b \rightarrow s\gamma$ constraint for higher values of $\tan\beta$. The upper bound on $m_{1/2}$ for $\tan\beta \gtrsim 50$ is clearly weaker, because of the rapid-annihilation regions.

Also shown in Fig. 2 in darker shading are the restricted parts of the strips that are compatible with the BNL measurement of $g_\mu - 2$ at the $2\text{-}\sigma$ level, if low-energy e^+e^- data are used to calculate the Standard Model contribution [17]. If this constraint is imposed, the range of $m_{1/2}$ is much reduced for any fixed value of $\tan\beta$, and in particular the upper bound on $m_{1/2}$ is significantly reduced, particularly for $\tan\beta \gtrsim 50$. However, there is in

³The droplets in the upper right of the figure are due to coannihilations when $\tilde{\tau}$ is sitting on the Higgs pole. Here this occurs at $\tan\beta = 45$.

general no change in the lower bound on $m_{1/2}$.

3 Improved Upper Limit on the LSP Mass

We now draw some conclusions from Fig. 2. Its implications for the allowed range of the LSP mass m_χ as a function of $\tan\beta$ are displayed in Fig. 3. As already mentioned, the upper limit is rather weak for $\tan\beta \gtrsim 50$ when $\mu > 0$. However, for $\tan\beta < 40$, we find the absolute upper bound

$$m_\chi \lesssim 500 \text{ GeV}, \quad (1)$$

to be compared with the range up to $\simeq 650$ GeV that we found with the old cosmological relic density constraint. Also shown in Figs. 2 and 3 is the strengthened upper bound on $m_{1/2}$ and m_χ that would apply if one used the $g_\mu - 2$ constraint. We find

$$m_\chi \lesssim 370 \text{ GeV}, \quad (2)$$

for all values of $\tan\beta$. Fig. 3(a) also shows the lower bound on m_χ as a function of $\tan\beta$, leading to

$$m_\chi > 108 \text{ GeV}, \quad (3)$$

for all values of $\tan\beta$, with the minimum occurring around $\tan\beta = 23$, when the $b \rightarrow s\gamma$ constraint begins to dominate over the Higgs mass constraint. As such, this lower limit depends on the calculation of m_h , for which we use the latest version of `FeynHiggs` [20]. This calculation has an estimated theoretical uncertainty ~ 2 GeV, and is very sensitive to m_t . The lower bound (3) would become > 86 GeV (with the minimum occurring at $\tan\beta \simeq 18$) if we used $m_t \simeq 180$ GeV in `FeynHiggs`, or > 84 GeV (with the minimum occurring at $\tan\beta \simeq 17$) if we allowed for a 2 GeV reduction in the calculated value for the nominal value of m_t .

We do not show the plot corresponding to Fig. 2 for $\mu < 0$, but we do show in Fig. 3(b) the corresponding lower and upper bounds on m_χ for $\tan\beta \lesssim 40$. We note again that the upper bound would rise rapidly for larger $\tan\beta$, due to the appearance of a rapid-annihilation funnel analogous to that appearing for $\tan\beta \gtrsim 50$ when $\mu > 0$. In the $\mu < 0$ case, there is no possibility of compatibility with $g_\mu - 2$ when the e^+e^- data are used. We find the following range for $\tan\beta \leq 30$:

$$160 \text{ GeV} < m_\chi < 430 \text{ GeV} \quad (4)$$

for $\mu < 0$, with the lower bound being provided by $b \rightarrow s\gamma$ for $\tan\beta > 8$.

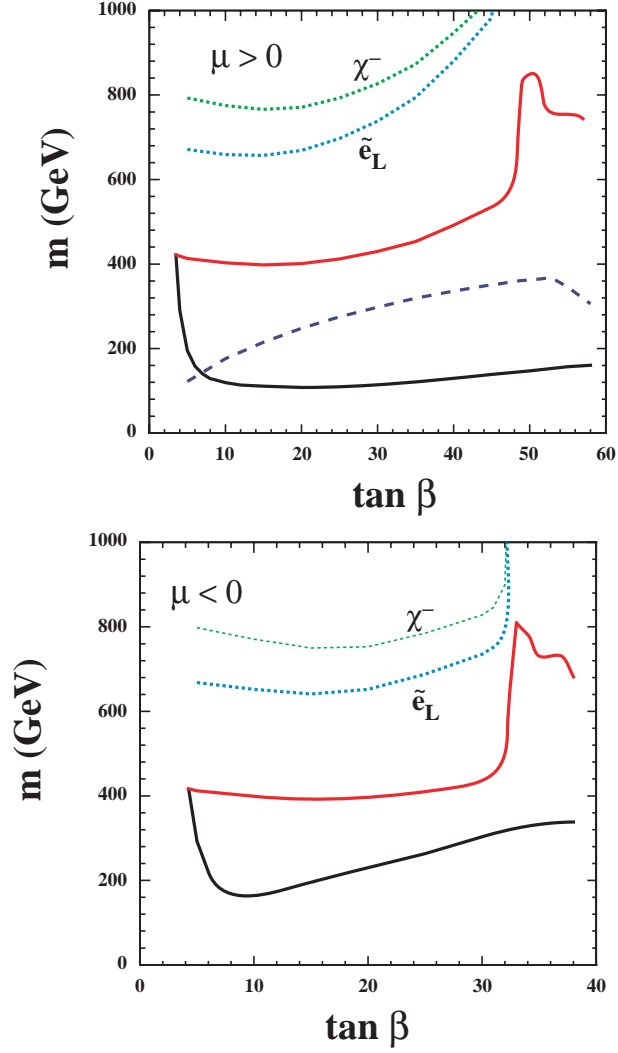


Figure 3: The ranges of m_χ allowed by cosmology and other constraints, for (a) $\mu > 0$ and (b) $\mu < 0$. Upper limits without (red solid line) and with (blue dashed line) the $g_\mu - 2$ constraint are shown for $\mu > 0$: the lower limits are shown as black solid lines. Note the sharp increases in the upper limits for $\tan \beta \gtrsim 50$, $\mu > 0$ and $\tan \beta \gtrsim 35$, $\mu < 0$ due to the rapid-annihilation funnels. Also shown as dotted lines are the \tilde{e}_L and χ^\pm masses at the tips of the coannihilation tails.

We note that the upper and lower limits meet when $\tan\beta = 3.5(4.3)$ for $\mu > (<)0$, implying that lower values of $\tan\beta$ are not allowed within our analysis of the CMSSM. This lower bound on $\tan\beta$ is strengthened to 7 if the $g_\mu - 2$ constraint is included.

4 Implications for Supersymmetric Phenomenology

The reduced upper limit on the sparticle mass scale improves the prospects for measuring supersymmetry at the LHC. Also, the fact that only a narrow strip in the $(m_{1/2}, m_0)$ plane is allowed for each value of $\tan\beta$ offers the possibility of determining $\tan\beta$ once $m_{1/2}$ and m_0 are known, e.g, from measurements at the LHC. We have discussed previously the sensitivity of $\Omega_\chi h^2$ to variations in the CMSSM parameters [21], and that analysis can be adapted to the present situation. Since the typical separation between strips with $\Delta(\tan\beta) = 5$ is $\Delta m_0 \simeq 25$ GeV and the width of a typical strip is $\Delta m_0 \simeq 5$ GeV, it would in principle be possible to fix $\tan\beta$ with an accuracy $\Delta(\tan\beta) \simeq 1$ using measurements of $m_{1/2}$ and m_0 alone for a fixed value of A_0 (taken to be 0 here). The required accuracy in $m_{1/2}$ is not very demanding, since the strips are nearly horizontal, but m_0 would need to be determined with an accuracy $\Delta m_0 \lesssim 5$ GeV. It is interesting to compare with the accuracies in m_0 , $m_{1/2}$ and $\tan\beta$ reported in [22] for the case $m_0 = 100$ GeV, $m_{1/2} = 300$ GeV and $\tan\beta = 2.1$. This value of $\tan\beta$ is not compatible with our analysis, but the expected accuracies $\Delta(m_0) \sim 10$ GeV and $\Delta(m_{1/2}) = 20$ GeV would already allow interesting crosschecks of the value of $\tan\beta$ extracted from a fit to the LHC data with that required by cosmology.

The strengthened upper bound (1) on m_χ may also have important consequences for linear e^+e^- collider physics [23]. At the tip of the coannihilation region, which corresponds to the upper bound in Fig. 3, we have $m_\chi = m_{\tilde{\tau}_1}$, with the $\tilde{\mu}_R$ and \tilde{e}_R not much heavier. Therefore, a linear e^+e^- collider with centre-of-mass energy 1 TeV would be able to produce these sleptons. This conclusion holds only if one restricts attention to the CMSSM, as studied here, ignores the focus-point region as also done here, and discards large values of $\tan\beta$. Moreover, we note that the left-handed sleptons are somewhat heavier at the tip of the CMSSM cosmological region: $m_{\tilde{\ell}_L} \gtrsim 700$ GeV, as shown by the pale blue dotted lines in Fig. 3, and the lightest chargino has $m_{\chi^\pm} \gtrsim 800$ GeV (green dotted lines). However, the strengthened upper limit on $\Omega_\chi h^2$ that has been provided by WMAP does strengthen the physics case for a TeV-scale linear e^+e^- collider, compared with [11].

5 Perspective

In general, the WMAP constraint on $\Omega_\chi h^2$ put supersymmetric phenomenology in a new perspective, essentially by reducing the dimensionality of the parameter space: one can now consider m_0 to be (almost) fixed in terms of the other parameters. The ‘Snowmass lines’ [24] now intersect the allowed cosmological region in just one (fuzzy) point each. The post-LEP benchmark points [25] have values of $\Omega_\chi h^2$ that lie above the WMAP range. However, most of them can easily be adapted, in the ‘bulk’ and coannihilation regions simply by reducing m_0 . An exception is benchmark point H, which was chosen at the tip of a coannihilation tail: WMAP would require this to be brought down to lower $m_{1/2}$, which would make it easier to detect at the LHC or a future linear e^+e^- linear collider. A more detailed update of the CMSSM benchmarks will be presented elsewhere.

Acknowledgments

We would like to thank H. Baer and A. Belyaev for helpful discussions. The work of K.A.O., Y.S., and V.C.S. was supported in part by DOE grant DE-FG02-94ER-40823.

References

- [1] C. L. Bennett *et al.*, arXiv:astro-ph/0302207; D. N. Spergel *et al.*, arXiv:astro-ph/0302209.
- [2] A. T. Lee *et al.* [MAXIMA-1 Collaboration], *Astrophys. J.* **561** (2001) L1 [arXiv:astro-ph/0104459]; C. B. Netterfield *et al.* [Boomerang Collaboration], *Astrophys. J.* **571** (2002) 604 [arXiv:astro-ph/0104460]; C. Pryke *et al.* [DASI Collaboration], *Astrophys. J.* **568** (2002) 46 [arXiv:astro-ph/0104490].
- [3] A. Melchiorri and J. Silk, *Phys. Rev. D* **66** (2002) 041301 [arXiv:astro-ph/0203200]; J. L. Sievers *et al.*, arXiv:astro-ph/0205387.
- [4] J. Ellis, J. S. Hagelin, D. V. Nanopoulos, K. A. Olive and M. Srednicki, *Nucl. Phys. B* **238** (1984) 453; see also H. Goldberg, *Phys. Rev. Lett.* **50** (1983) 1419.
- [5] J. R. Ellis, T. Falk, G. Ganis, K. A. Olive and M. Srednicki, *Phys. Lett.* **B510** (2001) 236 [arXiv:hep-ph/0102098].

- [6] J. R. Ellis, K. A. Olive and Y. Santoso, *New Jour. Phys.* **4** (2002) 32 [arXiv:hep-ph/0202110].
- [7] L. Roszkowski, R. Ruiz de Austri and T. Nihei, *JHEP* **0108** (2001) 024 [arXiv:hep-ph/0106334]; A. Djouadi, M. Drees and J. L. Kneur, *JHEP* **0108** (2001) 055 [arXiv:hep-ph/0107316]; H. Baer, C. Balazs and A. Belyaev, *JHEP* **0203** (2002) 042 [arXiv:hep-ph/0202076].
- [8] A. B. Lahanas, D. V. Nanopoulos and V. C. Spanos, *Phys. Rev. D* **62** (2000) 023515 [arXiv:hep-ph/9909497]; *Mod. Phys. Lett. A* **16** (2001) 1229 [arXiv:hep-ph/0009065]; *Phys. Lett.* **B518** (2001) 94 [arXiv:hep-ph/0107151]; V. Barger and C. Kao, *Phys. Lett.* **B518** (2001) 117 [arXiv:hep-ph/0106189]; R. Arnowitt and B. Dutta, arXiv:hep-ph/0211417.
- [9] J. Ellis, T. Falk, and K.A. Olive, *Phys. Lett.* **B444** (1998) 367 [arXiv:hep-ph/9810360]; J. Ellis, T. Falk, K.A. Olive and M. Srednicki, *Astr. Part. Phys.* **13** (2000) 181 [Erratum-ibid. **15** (2001) 413] [arXiv:hep-ph/9905481].
- [10] M. E. Gómez, G. Lazarides and C. Pallis, *Phys. Rev. D* **D61** (2000) 123512 [arXiv:hep-ph/9907261]; *Phys. Lett.* **B487** (2000) 313 [arXiv:hep-ph/0004028]; *Nucl. Phys. B* **B638** (2002) 165 [arXiv:hep-ph/0203131]; R. Arnowitt, B. Dutta and Y. Santoso, *Nucl. Phys. B* **B606** (2001) 59 [arXiv:hep-ph/0102181]. T. Nihei, L. Roszkowski and R. Ruiz de Austri, *JHEP* **0207** (2002) 024 [arXiv:hep-ph/0206266].
- [11] J. R. Ellis, G. Ganiis and K. A. Olive, *Phys. Lett. B* **474** (2000) 314 [arXiv:hep-ph/9912324].
- [12] M. Drees and M. M. Nojiri, *Phys. Rev. D* **47** (1993) 376 [arXiv:hep-ph/9207234]; H. Baer and M. Brhlik, *Phys. Rev. D* **53** (1996) 597 [arXiv:hep-ph/9508321]; A. B. Lahanas, D. V. Nanopoulos and V. C. Spanos, *Phys. Rev. D* **62** (2000) 023515 [arXiv:hep-ph/9909497]; H. Baer, M. Brhlik, M. A. Diaz, J. Ferrandis, P. Mercadante, P. Quintana and X. Tata, *Phys. Rev. D* **63** (2001) 015007 [arXiv:hep-ph/0005027]; A. B. Lahanas, D. V. Nanopoulos and V. C. Spanos, *Mod. Phys. Lett. A* **16** (2001) 1229 [arXiv:hep-ph/0009065].
- [13] J. L. Feng, K. T. Matchev and T. Moroi, *Phys. Rev. Lett.* **84** (2000) 2322; J. L. Feng, K. T. Matchev and T. Moroi, *Phys. Rev.* **D61** (2000) 075005; J. L. Feng, K. T. Matchev and F. Wilczek, *Phys. Lett.* **B482** (2000) 388.

- [14] M.S. Alam et al., [CLEO Collaboration], Phys. Rev. Lett. **74** (1995) 2885 as updated in S. Ahmed et al., CLEO CONF 99-10; BELLE Collaboration, BELLE-CONF-0003, contribution to the 30th International conference on High-Energy Physics, Osaka, 2000. See also K. Abe *et al.*, [Belle Collaboration], [arXiv:hep-ex/0107065]; L. Lista [BaBar Collaboration], [arXiv:hep-ex/0110010]; K. Chetyrkin, M. Misiak and M. Munz, Phys. Lett. B **400** (1997) 206 [Erratum-ibid. B **425**, 414 (1997)] [hep-ph/9612313]; T. Hurth, hep-ph/0106050; C. Degrossi, P. Gambino and G. F. Giudice, JHEP **0012** (2000) 009 [arXiv:hep-ph/0009337]; M. Carena, D. Garcia, U. Nierste and C. E. Wagner, Phys. Lett. B **499** (2001) 141 [arXiv:hep-ph/0010003]. P. Gambino and M. Misiak, Nucl. Phys. B **611** (2001) 338; D. A. Demir and K. A. Olive, Phys. Rev. D **65** (2002) 034007 [arXiv:hep-ph/0107329].
- [15] J. R. Ellis, T. Falk, K. A. Olive and Y. Santoso, Nucl. Phys. B **652** (2003) 259 [arXiv:hep-ph/0210205].
- [16] G. W. Bennett *et al.* [Muon $g - 2$ Collaboration], Phys. Rev. Lett. **89** (2002) 101804 [Erratum-ibid. **89** (2002) 129903] [arXiv:hep-ex/0208001].
- [17] M. Davier, S. Eidelman, A. Hocker and Z. Zhang, decays: arXiv:hep-ph/0208177; see also K. Hagiwara, A. D. Martin, D. Nomura and T. Teubner, arXiv:hep-ph/0209187; F. Jegerlehner, unpublished, as reported in M. Krawczyk, Acta Phys. Polon. B **33** (2002) 2621 [arXiv:hep-ph/0208076].
- [18] A. B. Lahanas and V. C. Spanos, Eur. Phys. J. C **23** (2002) 185 [arXiv:hep-ph/0106345].
- [19] The RunII D0 top group, see <http://www-d0.fnal.gov/Run2Physics/top/conf.html>.
- [20] S. Heinemeyer, W. Hollik and G. Weiglein, Comput. Phys. Commun. **124** (2000) 76 [arXiv:hep-ph/9812320]; S. Heinemeyer, W. Hollik and G. Weiglein, Eur. Phys. J. C **9** (1999) 343 [arXiv:hep-ph/9812472].
- [21] J. R. Ellis and K. A. Olive, Phys. Lett. B **514** (2001) 114 [arXiv:hep-ph/0105004].
- [22] I. Hinchliffe, F. E. Paige, M. D. Shapiro, J. Soderqvist and W. Yao, Phys. Rev. D **55** (1997) 5520 [arXiv:hep-ph/9610544].
- [23] T. Kamon, R. Arnowitt, B. Dutta and V. Khotilovich, arXiv:hep-ph/0302249.

- [24] B. C. Allanach *et al.*, in *Proc. of the APS/DPF/DPB Summer Study on the Future of Particle Physics (Snowmass 2001)* ed. N. Graf, Eur. Phys. J. **C25** (2002) 113 [arXiv:hep-ph/0202233].
- [25] M. Battaglia *et al.*, Eur. Phys. J. **C22** (2001) 535 [arXiv:hep-ph/0106204].